SPINE Volume 29, Number 21, pp 2389–2394
©2004, Lippincott Williams & Wilkins, Inc.

A Biomechanical Study of Regional Endplate Strength and Cage Morphology as It Relates to Structural Interbody Support

Thomas G. Lowe, MD,* Shukor Hashim, MD,† Lucas A. Wilson, BSME,*
Michael F. O'Brien, MD,‡ David A.B. Smith, MSc,* Molly J. Diekmann, BSc,* and
Julie Trommeter, BSME*

Study Design. An *in vitro* biomechanical investigation to quantify the endplates resistance to compressive loads, in the thoracic and lumbar spine. Comparisons were made to determine the regional strength of the endplate, the optimal size and geometry of interbody support, and the effects of endplate removal on structural strength.

Objectives. To biomechanically assess the regional variation of endplate strength in the thoracic and lumbar spine, the optimal geometry and cross-sectional area for structural interbody support, and endplate preparation techniques with respect to endplate failure or subsidence.

Summary of Background Data. Anterior column interbody support plays an important role in spinal reconstruction. Subsidence of interbody structural support is a common problem and may be related to regional weakness of the endplate, the size and/or geometry of structural support, and the preparation of the endplate. Biomechanical data related to these issues should be of importance to spine surgeons and reduce the risk of subsidence and its inherent complications.

Methods. The indentation tests were performed in three subgroups, each with a different set of test variables. The first test consisted of 65 vertebrae at six different endplate test positions using a 9.53-mm diameter indenter. The second test was performed on 48 vertebrae at a central endplate test site using three hollow and two solid cylindrical indenters of varying diameter. The third test was done using 24 vertebrae with the endplate intact, partially removed, or fully removed. All tests were run using human cadaveric specimen using both the superior and inferior endplates. The maximum load to failure (MLF) was determined for each test performed.

Results. For all levels tested, the highest MLF occurred in the posterolateral region of the endplate. The lowest value occurred in the central and anterocentral regions for levels T7–L5 and T1–T6, respectively. Hollow indenters with a small diameter had the lowest MLF, whereas solid large-diameter indenters had the highest MLF. The ultimate compressive strength for all hollow indenters was significantly higher than all solid indenters. There was a significant reduction in the endplate strength with the complete removal of the endplate.

Conclusions. The posterolateral region of the endplate provides the greatest resistance to subsidence while the central region provides the least resistance. A larger-diameter solid support has the greater MLF and the lower the risk of subsidence, suggesting a more efficient transfer of force to the endplate with the hollow indenters. Parameters such as the geometry of structural support and the position and preparation of the endplate can influence the resistance of an interbody support to subside. Partial removal of the endplate may provide both, for adequate mechanical advantage and a highly vascular site for fusion.

Key words: interbody support, subsidence, anterior column, endplate, biomechanics, thoracic, lumbar. **Spine 2004;29:2389–2394**

Anterior column interbody support plays an important role in spinal reconstruction. It is often necessary to achieve appropriate sagittal alignment, facilitate coronal deformity correction, create a load-sharing construct with anterior or posterior instrumentation, and provide an optimal mechanical and biologic environment for fusion. Along with the intrinsic benefits associated with the use of interbody support, there are several possible complications that can be associated with the use of interbody support in anterior column reconstruction. The most common of these problems is subsidence of the interbody support into the bony anatomy of the vertebral body, which can lead to segmental kyphosis, loss of anterior column support, pseudarthrosis, progressive deformity, and failure of anterior or posterior instrumentation. It is hypothesized that subsidence of interbody support may be affected by many factors, including regional strength of the endplate, endplate removal, and the size and geometry of the interbody spacer. There are conflicting data in the literature pertaining to optimal endplate position and preparation, and interbody support geometry.[1–5] Understanding how these factors influence the biomechanical interface between the endplate and support would be very helpful clinically, providing a framework for choosing the support, placing the support, and the intraoperative preparation of the endplate. Such information could reduce the risk of subsidence, the loss of segmental lordosis, and instrumentation failure.

The purpose of this study was: 1) to assess the regional variation of endplate strength in the thoracic and lumbar

From the *Woodridge Spine Center, Wheat Ridge, CO; †Kuala Lumpur Hospital, Malaysia[1]; and ‡Miami Children's Hospital, Miami, FL.
Acknowledgment date: October 23, 2003. Acceptance date: December 1, 2003.
The manuscript submitted does not contain information about medical device(s)/drug(s).
No funds were received in support of this work. No benefits in any form have been or will be received from a commercial party related directly or indirectly to the subject of this manuscript.
Address correspondence and reprint requests to Thomas G. Lowe, MD, 3550 Lutheran Pkwy West, Suite 201, Wheat Ridge, CO 80033; E-mail: woodridgespine@aol.com

spine, and determine if an optimal position(s) exists for anterior column interbody support; 2) to assess the optimal cage geometry (hollow *vs.* solid) and cross-sectional area with respect to vertebral endplate failure; and 3) to determine the effect of full or partial removal of the cortical endplate on the structural strength of the endplate.

Materials and Methods

The indentation tests were performed in three subgroups, each with a different set of test variables. The first test consisted of using 65 vertebrae at six different endplate test sites using a 9.53-mm diameter indenter. The second test was performed on 48 endplates at a central test site using three hollow and two solid cylindrical indenters of varying size. The third test was done using 24 vertebrae with the endplate intact, partially removed, or completely removed. All tests were run on human cadaveric specimen using both the superior and inferior endplates. The maximum load to failure was determined for each test performed.

Phase 1: Regional Endplate Strength. Sixty-five disarticulated human vertebrae from T1 to L5 were obtained from 5 fresh cadaveric specimens with a mean age of 48 years (range, 32–57 years). The specimens used in this study were obtained from donors free of medical or metabolic bone diseases. Bone densitometry measurements were obtained ranging from 0.794 to 0.909 g/cm^3, using a Hologic Bone Densitometer QDR-1000/W (Hologic Inc., Bedford, MA). The vertebrae were disarticulated and the posterior elements were removed, leaving 5 mm of each pedicle. Both the superior and inferior discs were removed from each vertebra, leaving the endplate and vertebral body intact. Each vertebra was then potted in DynaCast Green Epoxy (Kindt-Collins Corp., Cleveland, OH). A thin layer of cellophane was placed between the vertebra and epoxy to ensure that the opposing endplate did not contact the epoxy. Care was taken to pot the vertebrae so that the endplates were perpendicular to the planned direction of loading.

Compressive tests were performed with an MTS 809 Biaxial Servohydraulic Biomechanical Testing System (MTS Corp., Minneapolis, MN). A solid steel rod indenter with a diameter of 9.53 mm was used for all testing, so that the deformation of the steel would be negligible to that of the endplate. The rod size was chosen because it is similar to a small-diameter cage and allowed for testing at specific regions of the endplate. The indenter was secured in such a way as to ensure that the load from the indenter would be applied perpendicular to the endplate of the specimen, with the load cell under the potted vertebra. The maximum load to failure (MLF) of six different endplate locations, lateral (L), anterior lateral (AL), posterior lateral (PL), central (C), anterior central (AC), and posterior central (PC), on both superior and inferior endplates, was determined (Figure 1).

A compressive preload of 70 N was applied to the endplate. Specimens were then loaded in displacement control to failure at a rate of 25.4 mm per minute. Load and axial displacement data were recorded at a rate of 10 Hz. The MLF was calculated for each test. Student's *t* test' was used for statistical analysis and significance as accepted with a P value < 0.05.

The tests were categorized based on whether there was a previous test performed in close proximity, which might affect the MLF. The first test performed on each endplate was designated as "primary." As seen in Figure 2, "secondary" tests were defined as any test that was performed at an immediately adjacent location to a previous test site (*e.g.*, anterior-central and anterolateral or central after any other location had been tested). Adjacent positions were defined as test sites that were within one indenter diameter of a previously performed test. "Tertiary" tests were defined as tests performed at distances greater than one indenter diameter from the primary test. The

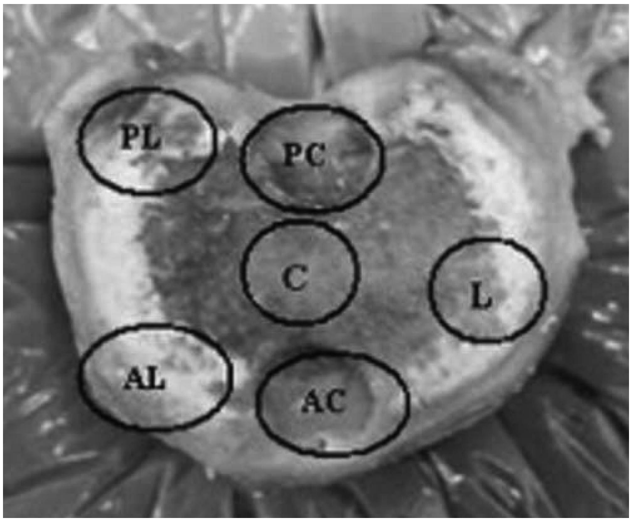

Figure 1. The six different endplate locations tested on for regional compressive strength using a 9.53 mm diameter indenter. Lateral (L), anterior lateral (AL), posterior lateral (PL), central (C), anterior central (AC), and posterior central (PC) are all shown.

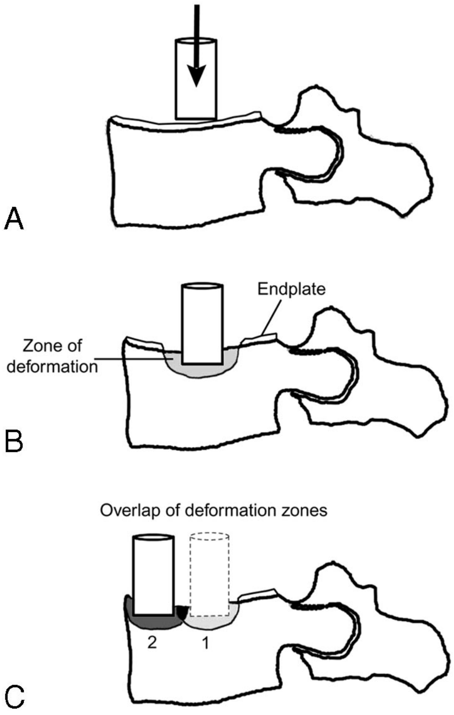

Figure 2. **A**, the perpendicular direction of the compressive load applied to the vertebral endplate by the indenter. **B**, the zone of deformation of the endplate created by the indenter. **C**, the overlap of deformation zones applied by the "primary" and "secondary" compression tests by the indenter.

Figure 3. Indenters used in compression testing. Hollow indenters of 9.53, 12.70, and 19.10 mm diameter and solid indenters of 9.53 and 12.70 mm diameters are shown.

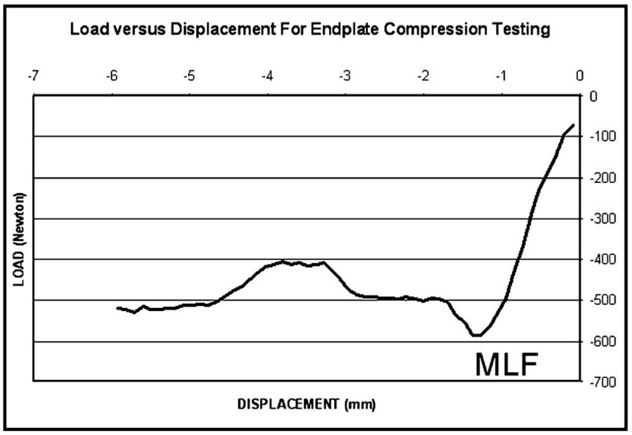

Figure 4. A representative Load-Displacement graph. Shown for test at left lateral position of T4 vertebra, MLF of 587 N, at 1.37 mm of displacement.

number of positions tested for each endplate depended on the area of the endplate. Analysis of primary, secondary, and tertiary tests showed that the MLF of secondary tests were statistically lower than primary and tertiary tests in the same region suggesting adjacent structural damage and reduced loads to failure of the endplate. As a result, secondary tests were not used in the data set.

Phase 2: Indenter Geometry. For this phase, 48 fresh disarticulated cadaveric vertebrae (age range, 40–50 years) were prepared in the same fashion as for Study 1. Bone density ranged from 0.820 to 0.899 g/cm^3, using a Hologic Bone Densitometer QDR-1000/W (Hologic Inc). A compressive load was applied in the same manner as the previous phase of the study. All tests were performed on the central region of the superior and inferior endplates. The tests were perform using three hollow indenter with major diameters of 9.53 mm, 12.70 mm, and 19.10 mm and a wall thickness of 1 mm, and two solid indenters with diameters of 9.53 mm and 12.70 mm (Figure 3). These hollow indenters approximate the geometric dimensions of currently available titanium mesh cages. In addition to the MLF, the ultimate compressive stress (UCS) was calculated for each test.

Phase 3: Endplate Preparation. Twenty-four disarticulated human vertebrae from T4–L5 were obtained from 2 fresh cadaveric specimens and used in the evaluation. The vertebrae were assigned using a randomization schedule to three different tests. There were three different testing modes: 1) fully intact endplate, 2) removal of the anterior third of the endplate, and 3) removal of the entire endplate. The cortical endplate was removed using a Dremel 770 Cordless MultiPro Tool with a small burr bit (Dremel, Racine, WI). Both the superior and inferior endplates were used and the vertebrae were potted as in phase 1. A 9.53-mm diameter solid steel indenter was used for all testing. The compressive load was centered on the sagittal plane and two thirds the way from the anterior cortex of the endplate. The specimen was tested in displacement control to failure at a rate of 25.4 mm/min and the load/displacement data were recorded at a rate of 10 Hz. The MLF was calculated for each test, and Student's *t* test was used for statistical analysis.

■ Results

For each test, the MLF was determined to be the maximum load following the linear region of the load-displacement curve, which was also used to determine the UCS for the geometry phase. The UCS was calculated as the MLF divided by the surface contact area of the indenter and the endplate. All the endplates failed with an indenter excursion between 1 and 3 mm. A typical load-displacement curve for all phases is shown in Figure 4. There was no significant difference between the inferior and superior endplates for all tests performed; therefore, both sets of data were combined for analysis.

Phase 1: Regional Endplate Strength

The data were broken down into three regions: upper thoracic (T1–T6), lower thoracic (T7–T12), and lumbar (L1–L5). Posterolateral position had the highest mean MLF throughout each region of the spine (Table 1). In the upper thoracic spine, the position with the next great-

Table 1. Results for the Position Testing and MLF

	Upper Thoracic				Lower Thoracic				Lumbar			
	n	Mean MLF (Newtons)	SE (Newtons)	% of Posterolateral	n	Mean MLF (Newtons)	SE (Newtons)	% of Posterolateral	n	Mean MLF (Newtons)	SE (Newtons)	% of Posterolateral
Posterolateral	19	874	41	100	14	782	95	100	8	1032	91	100
Anterolateral	13	602	81	69	15	585	62	75	11	715	75	69
Lateral	14	756	45	86	18	675	42	86	4	860	50	83
Central	6	631	128	72	7	485	93	62	4	596	75	58
Posterocentral	7	749	45	86	14	693	57	89	5	659	51	64
Anterocentral	10	550	50	63	14	692	61	89	8	751	24	73

Table 2. Results of the Indenter Size and Geometry

	Diameter (mm)	Test Group	n	Mean (SE) MLF (Newtons)	% of 19.10 mm Hollow Indenter	P	Mean (SE) UCS (Newtons/mm^2)	% of 12.70 mm Hollow Indenter	P
Hollow	9.53	1	19	1113 (128)	50	<0.001	53.2 (6.7)	92	0.553
	12.70	2	17	1646 (130)	74	0.037	57.8 (4.6)	100	—
	19.10	3	18	2238 (236)	100	—	51.3 (6.3)	89	0.366
Solid	9.53	4	27	1428 (121)	64	0.005	20.0 (1.7)	35	1.7E-7
	12.70	5	16	2200 (173)	98	0.899	17.4 (1.4)	30	7.9E-6

est resistance to compressive loads was the lateral and posterocentral; these values approached significance as compared to the posterolateral position ($P = 0.063$ and $P = 0.056$). In the lower thoracic vertebrae, the posterolateral position had a significantly higher mean MLF value compared with the next strongest positions of posterocentral and anterocentral ($P = 0.046$ and $P = 0.044$). In the lumbar region, the posterolateral position was followed by the lateral position, with marginal significance ($P = 0.128$). The central position provided a baseline mean MLF in both the lower thoracic and lumbar regions ($P < 0.005$), while the anterocentral provided the baseline upper thoracic region ($P < 0.001$).

Phase 2: Indenter Size And Geometry

The results for the indenter geometry portion of the testing are presented in Table 2. The indenters with the highest mean MLF values were the 19.10-mm diameter hollow and 12.70-mm diameter solid indenter, which produce very comparable peak loads. There was a significant decrease in mean MLF with Groups 1, 2, and 4 as compared with Groups 3 and 5 ($P < 0.037$ and $P < 0.016$). The mean UCS values for the hollow indenters tested showed substantially higher values of more than 250% of the solid indenters. This suggests a more efficient transfer of force to the endplate with the hollow indenters than with the solid indenters.

Phase 3: Endplate Preparation

The results for the lumbar and thoracic region tests produced very similar results and were combined for data analysis and are summarized in Table 3. There was a sequential decrease in the mean MLF that corresponded to the increased removal of the anterior portion of the endplate. The mean MLF for the fully removed cortical endplate was significantly lower than each of the other testing modes ($P < 9.3 \times 10^{-5}$). There was no significant difference in mean MLF between the intact endplate and the partially removed endplate. However, the partial removal of the endplate did suggest a minor decrease in the resistance of the endplate to compressive loads.

Table 3. Results of the Endplate Preparation and MLF

Test Mode	n	Mean (SE) MLF (Newtons)	% of Intact Test
Intact endplate	15	510.7 (34.1)	—
Anterior removed	17	469.7 (29.3)	92.0
Fully removed	15	312.5 (16.6)	61.2

Discussion

Phase 1: Regional Endplate Strength

When anterior column support is necessary, strategic positioning of the interbody spacer is required to take advantage of the strongest regions of the endplate. Kumar and Doherty noted that the posterolateral and posterocentral regions were significantly stronger than the rest of the vertebral endplates.[4] In their study, the zone of maximum strength extended as much as 4 mm centrally onto the endplate from the periphery. However, this study was only performed from L4–S1, with a 0.0625-inch diameter indenter, which does not represent the typical geometry of an interbody support. Additional investigations have reported similar results while using relatively small diameter (<3 mm) or limited to smaller regions of the spine.[2,3,5] The larger-diameter indenter used in this study suggests that the posterolateral endplate just anterior to the pedicle is the strongest portion of the endplate for both the thoracic and lumbar vertebrae. This is consistent with the biomechanical data presented by Kumar and Doherty from cadaveric lumbar and sacral testing.[4] It has been reported that the most dense area of the endplate is posterolateral near the pedicle base and the bone mineral density of the center position (350–450 mg/cm^3) is significantly lower than the periphery (600–700 mg/cm^3).[6] Perhaps the additional cortical bone at the base of the pedicle is responsible for the greater strength of the posterolateral endplate.

Data from this study suggest that the best endplate region to place structural interbody support appears to be the posterolateral, lateral, and posterior-central positions in the thoracic spine, and additionally the anterolateral position in the lumbar spine. This may be of significant clinical importance when using PLIF or TLIF techniques where smaller size cages are used. In that case, placing the cages posterolaterally and endplate removal anteriorly to facilitate an ideal fusion bed maximize structural support.

Phase 2: Indenter size and geometry

Total endplate coverage area has been shown to affect compressive strength suggesting that greater than 30% of the endplate should be prepared for grafting.[1] In a human cadaveric biomechanical study using titanium mesh cages (19-mm and 25-mm diameters), with and without end-rings, Hasegawa *et al* showed that, in compression, larger interbody cages had greater maximum loads to failure of the endplates than those with smaller cages.[3] The "end-ring" increased the bearing cortical surface area and contributed to a higher MLF for both the large and small cages.

In our study, the clinically important results are that for a given diameter, a solid spacer resulted in a higher mean MLF than a hollow spacer. However, using a larger-diameter hollow spacer can achieve a similar mean MLF as a smaller solid spacer. In this way, a hollow spacer may be optimized by increasing its diameter without increasing the risk of endplate subsidence and maximizing fusion potential by allowing more space for bone graft within the spacer.[1] When a smaller-diameter spacer is required because of anatomic constraints, a solid spacer may be required to optimize the MLF with placement of the graft around the spacer. The increased values for the mean UCS (MLF/cross-sectional area) of the hollow spacer is of biomechanical interest because it implies a more efficient and complex force transfer mechanism to the endplate. Allowing for higher forces to be sustained per unit area of spacer-endplate contact. This implies that a large-diameter hollow cage may represent the best combination of maximizing graft area, and minimizing endplate subsidence by providing maximum cross-sectional contact between the interbody support (cage) and the vertebral endplate.

Phase 3: Endplate Preparation

The contribution of the vertebral endplate to anterior interbody construct strength has been debated in the literature.[5,7] Endplate removal has been assumed to weaken the compressive strength of the vertebral body. No clear compromise has been established between the need to maintain vertebral endplates for anterior column support and endplate removal to improve vascularity for fusion enhancement. Accordingly, some surgeons remove the cortical vertebral endplate to improve vascularity for graft consolidation while others leave the vertebral endplate intact fearing structural anterior interbody support subsidence.

Biomechanical studies investigating interbody structural support subsidence after removal of varying amounts of endplate have produced inconsistent results.[5,7] Oxland *et al*, in a recent study, noted a 66% drop of the intact endplate failure load in indenter testing with a 3-mm hemispherical indenter.[5] Hollowell *et al* performed an analysis of thoracic cadaveric human vertebrae and concluded that preservation of vertebral endplate may not offer a significant biomechanical advantage in reconstructing the anterior column, and the titanium cage provided the greatest resistance to axial load.[7] Grant *et al*[2] and Lim *et al*[8] have highlighted the structural support provided by the endplates and the importance of maintaining their integrity to minimize the risk of graft subsidence. McBroom *et al* concluded that removal of the cortical endplate was associated with approximately a 10% reduction in vertebral load to failure.[9] Rockoff *et al* reported that the endplate contributes 45% to 75% of the peak strength of the vertebral body during compressive loading.[10] Approximately 40% of the load is transmitted *via* the trabecular bone beneath the cortical endplate. With a more representative investigation, we have confirmed this, with the decrease of nearly 39% in compressive strength with the complete removal of the endplate. However, there was a marginal decrease in endplate compressive strength with the removal only the anterior third of the endplate. This further reinforces the concept of regional strength and may provide a biomechanical compromise for the removal of weaker endplate positions to increase fusion rates. The partial removal of the endplate and placement of the interbody support on the remaining portion of the endplate may produce a structurally robust and highly vascular environment for fusion.

The data provided in this study present useful biomechanical information that can facilitate clinical decision-making regarding surgical techniques for providing anterior structural support. A large spacer with a hollow configuration that can engage the periphery and can be filled with graft material is probably ideal. However, if smaller spacers are preferred, then perhaps a solid spacer placed in a posterolateral or lateral position would optimize the biomechanical environment for construct success allowing for graft material to be placed around the spacer. Issues regarding cage size and geometry as well as placement in the interbody space are usually based on segmental sagittal or coronal deformities being addressed. For instance, if there has been symmetric collapse of a disc and the segmental lordosis has been lost, a tapered, large-diameter cage would be the best solution for treating the anterior column deficiency by allowing maximum restoration of lordosis and distraction of the interdisc space, which would facilitate foraminal nerve root decompression by an indirect means. If, however, scoliosis is the primary reconstructive goal, smaller, solid spacers placed in the posterolateral position in the concavity of the deformity may be the best strategy. This allows direct reduction of the deformity by compression of the convexity and provides the ability to gain additional correction by cantilever techniques. Care must be taken to place the cages along the lateral and posterolateral endplate to prevent subsidence and loss of correction and/or mechanical advantage when convex compression is performed. This will allow maximum mechanical advantage for correction using the strongest endplate regions and allow sufficient grafting surface to achieve fusion. Removal of small non–load-bearing areas of the endplate and placement of the morselized bone graft on the convexity side of the interdisc space under compression will maximize the biologic environment for fusion.

Care should be taken to provide a reasonable cross-sectional interface between the cage and the endplates. As previously mentioned, some cages such as carbon fiber cages typically have wall thickness sufficient to provide sufficient cross-sectional endplate-bearing surfaces. Titanium cages, however, will likely require the insertion of an "end-ring" at each end of the cage to provide adequate cross-sectional bearing surface required to prevent subsidence even when the cage engages the periphery of the endplates.

When performing posterior interbody support, either *via* a PLIF or a TLIF, one is restricted to a smaller area for placement of the cage, requiring smaller cages of either a solid or a hollow design. Because of this smaller diameter, care must be taken to maximize the endplate bearing surface area and optimize the placement of the cage to provide successful interbody support. If reestablishing lordosis is a prime concern, two strategies can be used to achieve this goal. Either two small-diameter spacers can be placed in the anterolateral position bilaterally to maximize the ability to achieve cantilever correction by compression, thus achieving lordosis, perhaps at the expense of neuroforaminal narrowing. However, if the anulus is pliable, then achieving maximum distraction between the posterior margin of the vertebral bodies and placing two small-diameter spacers in the posterolateral position would allow engagement of the strongest parts of the posterior endplate and provide a fulcrum with the capability of maximizing lordosis and avoiding foraminal stenosis. Whichever technique is used, care must be taken to check the neuroforamen for nerve root compression after performing a cantilever correction as described.

■ Conclusions

The posterolateral region of the endplate was the strongest in both thoracic and lumbar spines followed by lateral and posterocentral regions in the thoracic spine and additionally the anterolateral region in the lumbar spine.

- The central region of the endplate was 38% weaker than the posterolateral position in both the thoracic and lumbar spine, which was a significant difference.
- Preservation of the entire or posterior third of the cortical endplate provides a significant mechanical advantage for anterior column support.
- For a given diameter, solid spacers resulted in a higher MLF than hollow spacers; however, using a larger-diameter hollow spacer can achieve a similar mean MLF as a smaller solid spacer.
- When a small spacer is required because of anatomic constraints, a solid spacer may be required to optimize the MLF.
- The mean endplate UCS for hollow spacers was 60% higher than for solid spacers, implying a more efficient force transfer mechanism to the endplate with hollow spacers, which allows higher forces to be sustained per unit area of spacer–endplate interface.

■ Key Points

- The posterolateral portion of the vertebral endplate just anterior to the pedicle appears to be the strongest.
- The central portion of the endplate has a thin cortex and provides little resistance to a compressive load.
- A large diameter hollow spacer that can engage the peripheral margins of the endplate and can be filled with bone graft material appears to be ideal.
- For a transforaminal lumbar interbody fusion (TLIF), small diameter solid spacers placed posterolaterally appear to be ideal, leaving room for placement of graft material anteriorly.

References

1. Closkey R, Parson R, Lee C, et al. Mechanics of interbody spinal fusion: analysis of bone graft area. *Spine* 1993;18:1011–15.
2. Grant P, Oxland T, Dvorak M. Mapping the structural properties of the lumbosacral vertebral endplates. *Spine* 2001;26:889–96.
3. Hasegawa K, Abe M, Washio T, et al. An experimental study on the interface strength between titanium mesh cage and vertebra in reference to vertebral bone mineral density. *Spine* 2001;26:957–63.
4. Kumar A, Doherty B. Biomechanical testing of vertebral endplates strength: a cadaver study. *NASS 8th Annual Meeting*, San Diego, 1993.
5. Oxland TR, Grant PJ, Dvorak MF, et al. Effects of endplate removal on the structural properties of the lower lumbar vertebral bodies. *Spine* 2003;23: 771–7.
6. Wenger KH, Pross A, Wilke HJ, et al. Bone mineral density of the vertebral endplates: an in vitro comparison of normal, degenerative, and osteoporotic. *International Society for the Study of the Lumbar Spine*, Kona, HI, 1999.
7. Hollowell JP, Vollmer DG, Wilson CR, et al. Biomechanical analysis of thoracolumbar interbody constructs: how important is the endplate? *Spine* 1996;21:1032–36.
8. Lim TH, Kwon H, Jeon CH, et al. Effect of endplate conditions and bone mineral density on the compressive strength of the graft-endplate interface in the anterior cervical spine fusion. *Spine* 2001;26:951–6.
9. McBroom RJ, Hayes WC, Edwards WT, et al. Prediction of vertebral body compressive fracture using quantitative computed tomography. *J Bone Joint Surg Am* 1985;67:1206–14.
10. Rockoff D, Sweet E, Bleustein J. The relative contribution of trabecular and cortical bone to the strength of human lumbar vertebrae. *Calcif Tissue Res* 1969;3:163–75.